

# Response of Building Structures to Blast Effects

Osman Shallan, Atef Eraky, Tharwat Sakr, Shimaa Emad

Department of Structural Engineering, Faculty of engineering, Zagazig University, Zagazig, Egypt

*Abstract—As a result of repeated terrorist incidents around the world that target important and military structures, blast loads have received great interest in recent years. This paper investigates, through numerical simulations, the effects of blast loads on three buildings with different aspect ratios. Finite element models of these buildings were developed using the finite element program AUTODYN. Blast loads located at two different locations and spaced from the building with different standoff distances were applied. The simulations have revealed that the effect of blast load decrease with increasing the standoff distance from the building and with variation the aspect ratios of the buildings there is no variation in the displacement of the column in the face of the blast load but with increasing the aspect ratio the effect of blast load decrease in other element in the building.*

**Index Terms—Blast load, Buildings, Aspect ratio, Standoff distance.**

## I. INTRODUCTION

Due to various accidental or intentional events, related to important structures all over the world, blast loads have received great interest in recent years. The interest in protecting infrastructure against terrorist attacks and blast hazards was strongly generated after the bombing of the Murrah Federal Building in Oklahoma City in April 1995. A second wave of attention was generated after the bombing of the Khobar Towers in Saudi Arabia in June 1996. Following September 11, 2001, attacks on New York City's World Trade Center (WTC), was the key event that raised a high interest level of protecting critical infrastructural targets against blast scenarios [1]. Designing and construction of public buildings to assure life safety against explosions is receiving a great attention from structural engineers [11]. An explosion is defined as a large-scale, rapid and sudden release of energy. The threat for a conventional bomb is defined by two equally important elements, the bomb size, or charge weight  $W$ , and the standoff distance  $R$  between the blast source and the target "Fig.1". For example, the blast occurred at the basement of World Trade Centre in 1993 has the charge weight of 816.5 kg TNT. The Oklahoma bomb in 1995 has a charge weight of 1814 kg at a standoff of 4.5m. As terrorist attacks may range from small letter bomb to the gigantic truck bomb as experienced in Oklahoma City, the mechanics of a conventional explosion and their effects on a target must be addressed [13]. B.M. Luccioni et al [11] studied the analysis of buildings collapse under blast loads. The problem analyzed corresponding to an actual building that has suffered a terrorist attack. The paper includes comparisons with photographs of the real damage produced by the explosive charge that validates the simulation procedure. Jun Li and

Hong Hao [8] studied development of a simplified numerical method for structural response analysis to blast load. It demonstrated that the proposed method with more than 90% savings in computational time, yields reasonable predictions of structural responses. The proposed method has great potentials for application in practice to model responses of large structures to blast loadings. Björn Zakrisson et al [19] studied numerical simulations of blast loads and structural deformation from near-field explosions in air. K.M.A. Sohel and J.Y. Richard Liewb [16] investigated the impact behavior of sandwich slabs which consist of a lightweight concrete core sandwiched in-between two steel plates inter-connected by J-hook connectors. Hailong Chen [4] carried out a structural model experiment on a buried scaled down reinforced concrete arch structure subjected to underground close-in explosions. Jun Li and Hong Hao [9] investigated numerically spall damage of generic reinforced concrete columns subjected to blast loads. Three-dimensional numerical models are developed to predict the concrete spalling under blast. F. Stochino and G. Carta [17] examined reinforced concrete beams subjected to blast and impact loads. Chengqing Wua et al [18] performed a 3-dimensional dynamic response and damage analysis of masonry and masonry in filled RC frame structures to blast induced ground excitations. A two-story masonry structure and two-story masonry in filled RC frame as well as a six-story RC frame filled with masonry wall were used as examples in the study. Numerical results indicated that with the same ground excitation, the most severe damage occurred in the two-story masonry structure while the six-story RC frame filled with masonry wall experienced least damage. In addition many researches handled the progressive collapse of buildings under the effect of blast load [5, 12, 15]. Ruwan Jayasooriya et al [6] studied the impact of near field explosions on the structural framing system and key elements such as columns and described the component material response. Serdar Astarlioglu and Ted Krauthammer [2] used a numerical study to investigate the response of a normal-strength concrete (NSC) column that was not designed for blast resistance subjected to four levels of idealized blast loads. Denis Kelliher and Kenneth Sutton-Swaby [7] combined the Monte Carlo method, used in many structural reliability algorithms, with a simplified but conservative progressive collapse structural model. This resulting algorithm was used to generate a dataset representing the percentage damage a ten story reinforced concrete building subjected to an explosive load of a given magnitude located randomly in the ground floor car park. Xiaoshan Lin et al [10] developed a finite element model for the simulation of the structural response of steel-reinforced

concrete panels to blast loading using LS-DYNA. Parametric study was carried out to investigate the effects of charge weight, standoff distance, panel thickness and reinforcement ratio on the blast resistance of reinforced concrete panels.

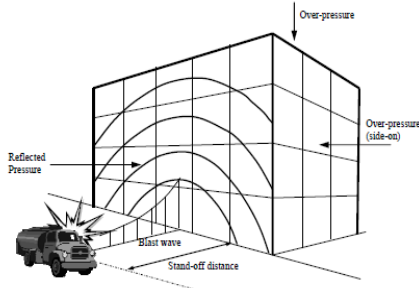


Fig.1: blast loads on a building [13]

This paper investigates the effect of blast loads on reinforced concrete buildings through the study two story buildings with three different aspect ratios. These buildings have aspect ratios 0.5, 1.0 and 1.5. The blast load location is also studied in two cases. In the first case the blast load located at different distances from the middle column and in the second case the blast load located at different distances from the corner column. It is assumed that the damage was caused by an explosive load equivalent to 1000 kg of TNT placed at 2.0 m height from the ground and at different distances from the buildings.

## II. AUTODYN MODEL

The finite element program AUTODYN is selected to model blast load effect on structures of the study. AUTODYN is an explicit analysis program designed for highly nonlinear dynamic problems [3]. AUTODYN has an efficient and fast single material high resolution Euler Flux Corrected Transport process for 2D and 3D blast problems. A feature of AUTODYN is its remapping technique where the output of a high resolution initial detonation stage is remapping as initial condition for the subsequent calculation stage. This allows modeling of the detonation process with very high grid resolution without increasing the computational demand. Detonation modeling in AUTODYN is two step processes. The first step involves the early time expansion of the explosive products in 1D using radial symmetry, which continues until a reflecting surface is reached. The output of the 1D analysis is then transmitted to the 3D domain that is generated separately. The analysis is run until the termination time.

### A. 1D ANALYSIS

The explosion is modeled using Jones-Wilkin-Lee Equation of State (JWL EOS) and the air is modeled as an ideal gas. The air was modeled as an ideal gas. The multi material Eulerian solver was used for both the explosive and the air. In AUTODYN the 1D simulation is modeled using 2D axisymmetric solver in the shape of a wedge. Only wedge inner and outer radius needs to be defined. The dimension of the wedge depends upon charge weight and location of pressure measurement. In the case of 1000kg TNT is

detonated in the air and pressure generated at a distance of 3m from the center of blast charge. The wedge length approximately equal to 3m (2.99m) is defined with radial symmetry (AUTODYN -2D) as shown in Fig.2 .The wedge is filled with explosive and air. The radius of the explosive was 0.527m. The start point for the wedge was 5 mm from the origin to avoid a zero thickness element at the origin. Although this correction reduced the volume of the explosive, the percentage reduction is negligible. A flow out boundary condition is defined at the end wedge. This boundary condition will allow pressure wave to go out of the domain without reflecting any pressure back to the domain [14].

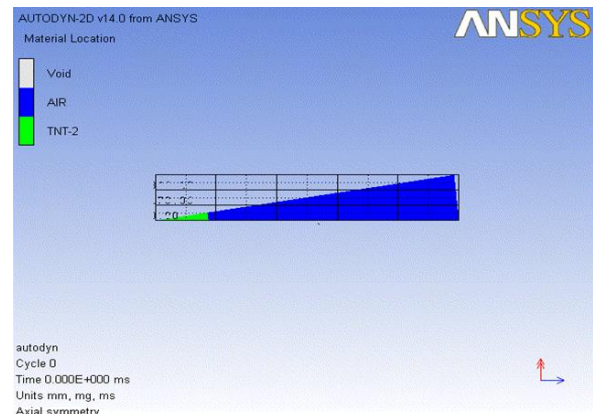


Fig.2: 1D wedge filled with TNT and air modeled with multi material Eulerian formulation.

### B. 3D ANALYSIS

The model is composed of the building and air volume occupied by the building. Air is modeled as an ideal gas. AUTODYN has a fast and efficient Euler Flux Corrected Transport (FCT) solver that was developed for blast applications. The output of the 1D analysis is transformed into the 3D domain and the start time of the 3D analysis was set equal to the end time of the 1D analysis. The output of the 1D analysis included multiple materials: air and explosion product gases. When the output was remapped to the single material 3D Euler-FCT domain, the explosion gases had to be converted to air defined in the 3D domain. The blast load is studied on three buildings with different aspect ratios in two cases as shown in Fig.3. Buildings A, B and C have an aspect ratio 0.5, 1.0 and 1.5 respectively. The three buildings have the same depth ( $D = 6$  m) with two bays in both longitudinal and transverse directions and with two story. The floor to floor story height of each level is 4.2 m. Rectangular columns sized 400 mm  $\times$  600 mm and beams in the longitudinal and transverse direction with depth = 600 mm and width = 400 mm. The slab thickness of the floor is 200 mm.

## III. MATERIAL PROPERTIES

The mechanical properties of the air, explosive and reinforced concrete will be illustrated.

### A. REINFORCED CONCRETE

Reinforced concrete elements can be modeled as a combination of concrete and steel elements jointed together

with the assumption of perfect bond, this type of model is prohibited for actual structures, as it requires a great number of elements. Moreover, the time step in explicit dynamic programs is directly related to the size of the elements. Elements of the dimensions of the actual reinforcement usually lead to extremely reduced time steps, making the analysis too slow. Taking into account the above considerations, an approximate material model for reinforced concrete was defined to simulate the behavior of reinforced concrete columns, beams and slabs that formed the resistant structure of the building. The model used is a homogenized elasto-plastic material similar to concrete models but with higher tension strength to take into account the collaboration of the reinforcement to resist tensile stresses. The mechanical properties of the homogenized model used for reinforced concrete are shown in Table (1). This concrete model with increased tension capacity was used for all reinforced concrete elements [2].

**TABLE (1) MECHANICAL PROPERTIES OF REINFORCED CONCRETE**

Parameter	Value
State equation	Linear
Reference density	2.750 g / cm <sup>3</sup>
Bulk modulus	3.527 E + 07 KPa
Strength model	Von Mises
Shear modulus	1.220 E + 07 KPa
Elastic limit	1.000 E + 04 KPa
Failure criteria	Principal stresses
Failure stress	1.000 E + 04 KPa

**B. EXPLOSIVE AND AIR**

A fluid with the properties presented in Table (2) was used to model the air.

**Table (2) JWL and ideal gas EOS parameters for explosive and air.**

JWL EOS for explosive		Linear polynomial EOS for air	
parameter	Value	parameter	Value
A(GPa)	371.2	C <sub>0</sub>	0
B(GPa)	3.231	C <sub>1</sub>	0
R1	4.15	C <sub>2</sub>	0
R2	0.95	C <sub>3</sub> = C <sub>6</sub>	0
ω	0.30	C <sub>4</sub> = C <sub>5</sub>	0.40
E <sub>o</sub> (GPa)	7.0	E <sub>o</sub> (GPa)	0.00025
ρ (Kg/ m <sup>3</sup> )	1630	ρ (Kg/ m <sup>3</sup> )	1.225
U (m/s)	6930		

**IV. RESULTS**

**EFFECT OF THE STANDOFF DISTANCE**

For the three building studied, the effect of blast load is studied at different distances from the building. These distances are a ratio from the width of the building. These

ratios are 0.25, 0.5, 1.0 and 1.5 times the width of the building. Blast load is studied in two cases, in the first case the blast load is located at different distances from the middle column C2 and in the second case the blast load is located at different distances from the corner column C1 as shown in Fig.3.

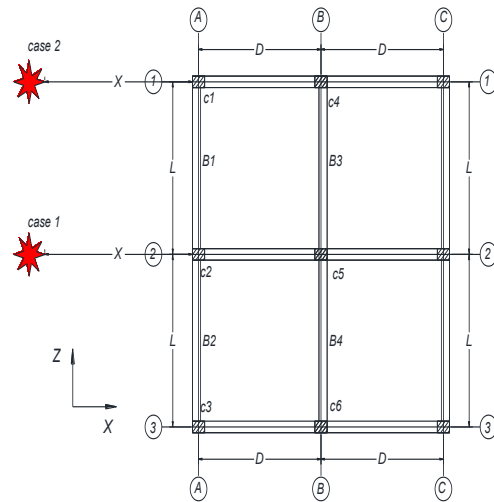


**Fig. 3 Plan of the building and Location of Blast.**

**1. BUILDING A**

The first building in the study is two story building with aspect ratio 0.50 (D= 6 m, L = 3 m) for which the blast effect is studied. As will be discussed later, two different cases of blast locations are studied as shown in Fig. 3. For each case, stand-off distances of 1.5, 3, 6, and 9 m shall be considered.

**CASE 1(SYMMETRIC LOADING)**

In this case the point of the blast load is located at different distances from the column C2. The blast load distances are 1.5, 3.0, 6.0, 9.0 m respectively. Fig.4 shows the deformed shape of the building due to detonation point at distance equal 1.5 m at time 100 msec. It is shown that the blast load causes a total failure of column C2. It is shown also that there is an uplift force on the floor. It is shown that the blast wave made a torsional force in the beam in the face of this blast wave. Fig.5 and 6 show the variation of reflected overpressure and temperature with time at mid height of column C1 due to blast load at distance equal to 1.5, 3.0, 6.0 and 9.0 m from column C2. It is shown that the arrival time of the blast load increases while the values of reflected overpressure and temperature decrease with increasing the distance from the detonation point. It is shown also that there are little differences between values of pressure when the detonation point at 1.5 m and at 3.0 m from the building, where the values of pressure are 9775 and 9343 Kpa and the temperature values are 4942 and 4938 °K. The case of 6m and 9m distance recorded more pronounced delay of arrival and more reduction of the values of peak pressures. The decay of pressure wave is also observed to be more steep in case of near distances (1.5 and 3 m) that of relatively far distances (6 and 9 m). It is also observed that the reflected overpressure decreases by 71.5% from the blast load at 1.5 m to blast load at 9.0 m.

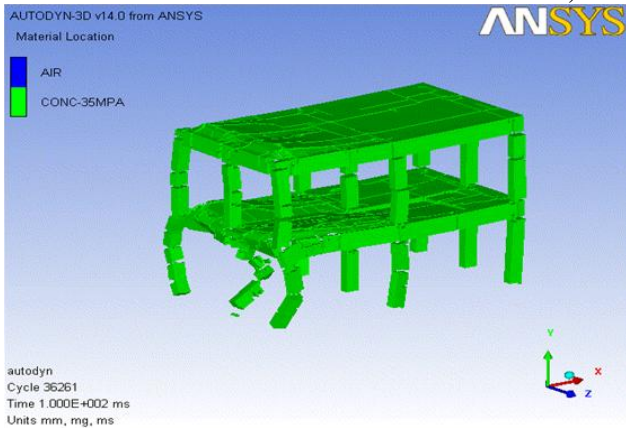


**Fig.4:** deformed shape of building A due to blast load at 1.5m from the middle column.

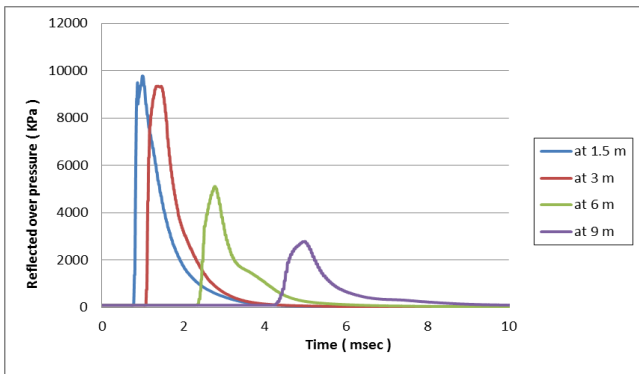


**Fig.5:** reflected overpressure histories at mid height of column C1 of building A - load case 1.

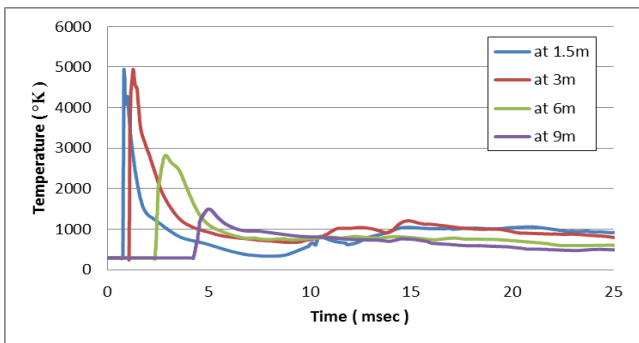


**Fig.6:** temperature histories at mid height of column C1 of building A - load case 1.

Fig.7 shows the variation of transverse (z-direction) displacements at mid height of column C1 due to blast load at distances 1.5, 3.0, 6.0 and 9.0 m from the building. Displacements are increased with time during the time of observation. The relation is approximately linear between displacement and time. For all gauges in the building the problem stopped at 100 msec due to failure of most of the members of the building and after this time the total failure in the building will take place. It is observed that the fragments due to the failure of the column moving away from the building up to 0.8 m in z direction due to detonation point at 1.5m from column C2. It is shown that the z displacement of this column varied from 784, 544.2, 139.7 and 29.2mm due to detonation point at 1.5, 3.0, 6.0 and 9.0 m from the building respectively. It is shown that there are a big difference

between its displacement due to blast load at 1.5, 3.0 and 6.0, 9.0m where the displacement decreased by 96% .

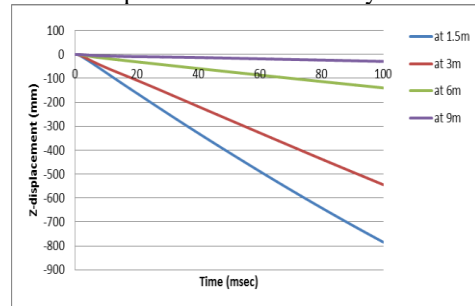


**Fig.7:** z-displacement histories of at mid height of column C1 of building A – load case 1.

Fig.8 shows the variation of lateral (x-direction) displacement at mid height of column C2 with time. It is shown that column C2 is more affected than any part of the building as it faces directly the blast point. The x-displacement as shown in the Figure increases linearly with time. It is shown that the displacement of this column due to blast load varied from 1649.3, 408, 5.76 and 1.71 mm due to blast load at 1.5, 3.0, 6.0 and 9.0m from this column respectively at time equal to 100 msec. It is also observed that there are big difference between the values of displacement of column due to blast load at 1.5m and 3.0m. It is shown also that with increasing the distance of blast load from the building there are little differences in its displacement.

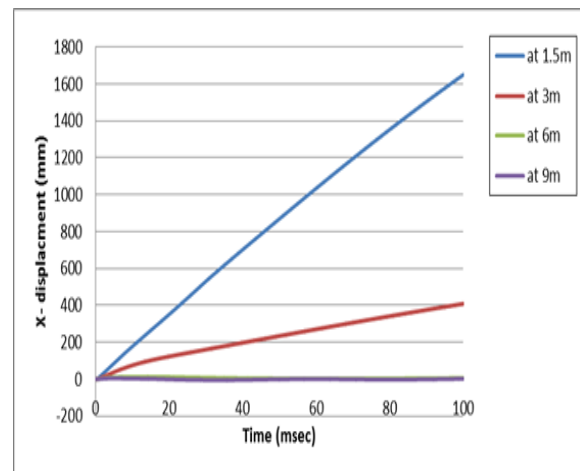


**Fig.8:** x-displacement histories of at mid height of column C2 of building A - load case 1.

### CASE 2(SKEW LOADING)

In this case the point of the blast load is located at different distances from column C1 at the corner of the building. Fig.9 shows the deformed shape of the building due to detonation point at 1.5 m from column c1 at time 100 msec. It is shown that the blast load caused a total failure of column C1 while the reflected waves cause large deformation in the facing row and second row columns. Uplift pressure effect is also clear in the region of slab near the explosion point.

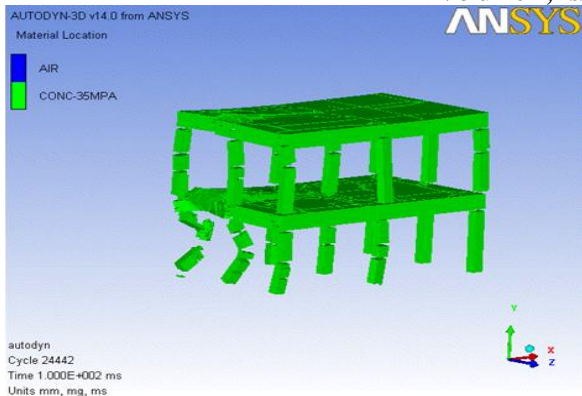


Fig.9: deformed shape of building A due to blast load at 1.5m from the corner column.

Fig. 10 shows the variation of lateral, x-displacement at mid height of column C1 with time. Displacements are increased with time during the time of observation. The relation is approximately linear between displacement and time. While positive pressure acts on column C1 for case of stand-off distance 1.5 and 3 m, the case of 6 and 9 m produces negative pressure (in opposite direction) with very small values while with increasing the distance of the blast load from the building the arrival time increase and the negative phase of pressure start to appear. The differences in pressure values are also observed to be significant with the variation of the stand-off distance between 1.5, 3 and 6 m while the 6 and 9 m stand-off produces relatively similar values of pressure. It is shown that the fragments due to the failure of the column moving away from the building up to 1.6 m in x direction due to detonation point at 1.5m from column C1. It is shown in this case that column C1 more affected than any part of the building. It is shown also the displacements in this case at 100 msec are 1583, 387, -1.83, -41.5 mm, where in case1 the displacements are 240, 57, 5.8 and -59.6 mm due to blast load at distance equal 1.5, 3.0, 6.0, 9.0 m from column C1 respectively. Fig.11 shows the variation of transverse z-displacement at mid height of column C2 with time. It is shown that displacement of this column varies from 824.4, 416.3, 94.2 and 16.1 mm, where in case 1 are 1649.3, 408, 5.76 and 1.71 mm due to blast load at 1.5, 3.0, 6.0 and 9.0 m from C1 respectively.

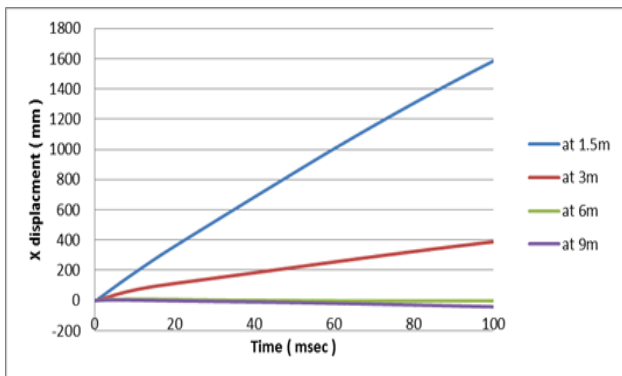


Fig.10: x-displacement histories of at mid height of column C1 of building A – load case 2.

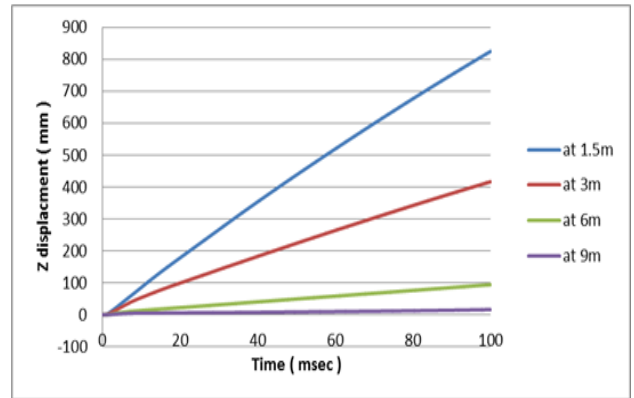


Fig.11: z-displacement histories of at mid height of column C2 of building A – load case 2.

Fig.12 shows the variation of transverse (z-direction) displacement of column C3 with time. It is shown that the displacement of this column due to blast load at distance 3m larger than the displacement of this column due to blast load at 1.5 m because the reflected overpressure from the column C2 decrease the blast load that reach to this column and this reflected pressure due to blast load at distance 1.5 m is bigger than that at 3.0 m due to the difference in the angle of incidence.

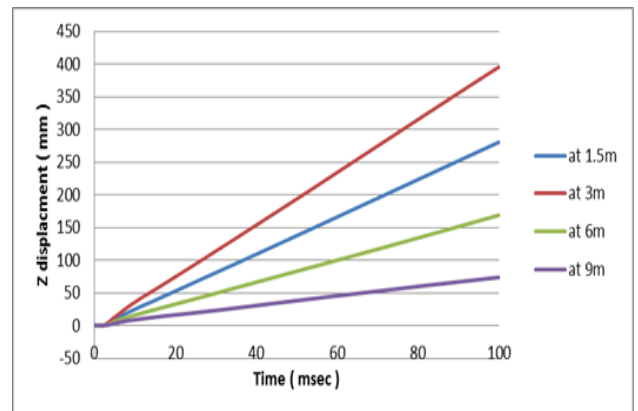


Fig.12: z-displacement histories of at mid height of column C3 of building A – load case 2.

## 2. BUILDING B

For the second building (building B), aspect ratio is changed to 1.0 by increasing the breadth of the building (L=6.0m), while the same depth (D=6.0m) is used. The two blast position cases and the four stand-off distances are applied and their results are investigated.

### CASE 1(SYMMETRIC LOADING)

Fig.13 shows the deformed shape of the building under the effect of blast load at 1.5 m from column C2. The figure shows that the effect of the blast load in the first bay of the building is larger than its effect in the second bay it is shown also that the first floor is more affected than second floor.

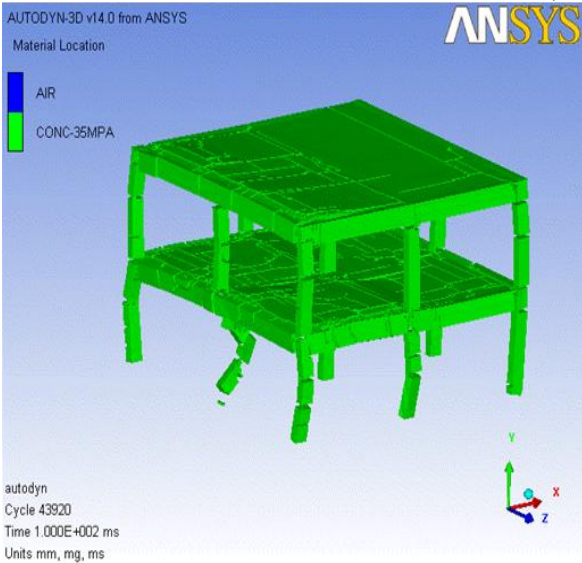


Fig.13: deformed shape of building B due to blast load at 1.5m from the middle column.

Fig.14 shows the variation of transverse z-displacement of column C1 with time. It is shown that the displacement in building B less than the displacement in building A where the displacement in building B varied from 394.4, 352.7, 140.4 and 34.6 mm where in building A varied from 784, 544.2, 139.7 and 29.2 mm due to detonation point at 1.5, 3.0, 6.0 and 9.0 m from the building respectively. It is shown also that with increasing the distance from the building there is no variation in displacement between two buildings.

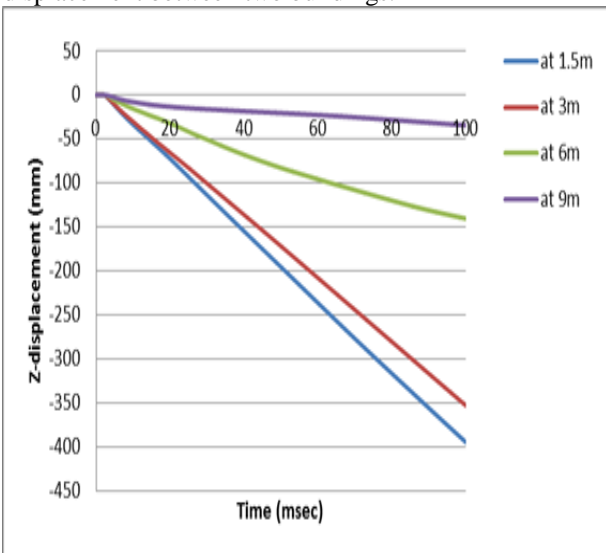


Fig.14: z-displacement histories of at mid height of column C1 of building B – load case 1.

Fig.15 shows the variation of lateral x-displacement of column C2 with time. It is shown that there are little differences in its displacements compared with building A due to the blast load in the face of this column and at the same distance in the two buildings. While displacements in building A are 1649.3, 408, 5.76 and 1.71 mm, the values of displacements in this building are 1580, 420, 6.6 and 2.8 mm due to blast load at 1.5, 3.0, 6.0 and 9.0m respectively.

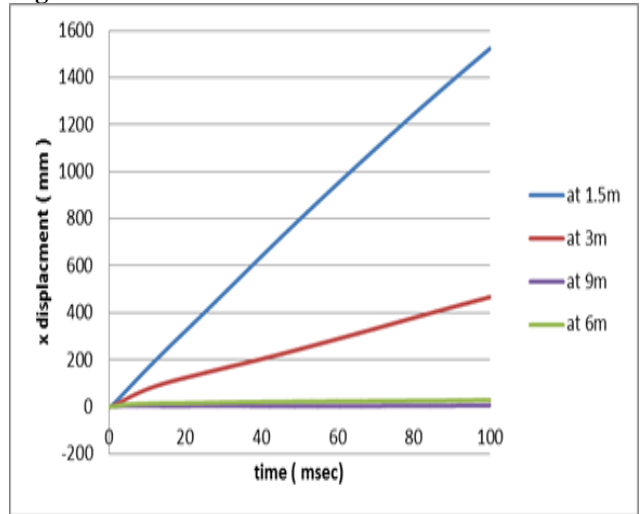


Fig.15: x-displacement histories of at mid height of column C2 of building B – load case 1.

CASE 2(SKEW LOADING)

Fig.16 shows the deformed shape of the building under the effect of blast load at 1.5 m from column C1 at time 100 msec. It is shown that there is a total failure in the column in the face of the blast load.

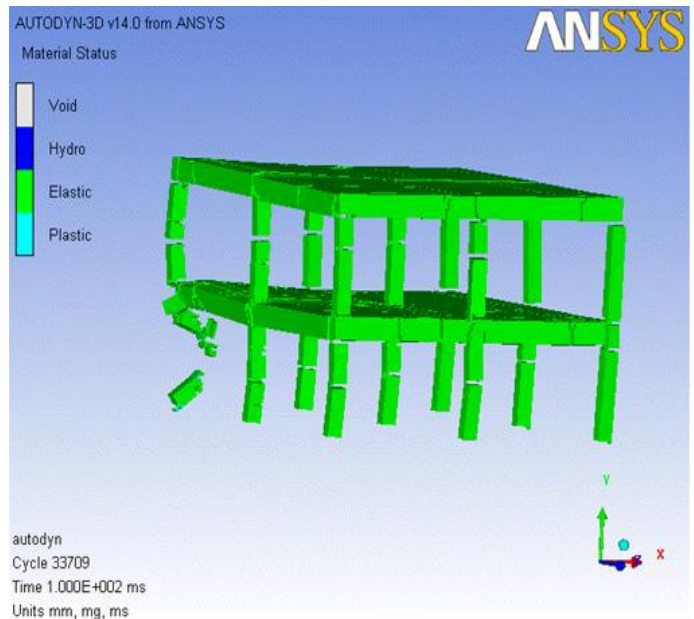


Fig.16: deformed shape of building B due to blast load at 1.5m from the corner column.

Fig.17 shows the variation of lateral x displacement of column C1 with time. It is shown that displacements of column C1 are approximately the same as that of building A. Same behavior is also observed leading to the conclusion that the aspect ratio does not affect the lateral displacement behavior of this column. This can be easily attributed to the column being facing the blast and exposed directly to its waves in all cases.

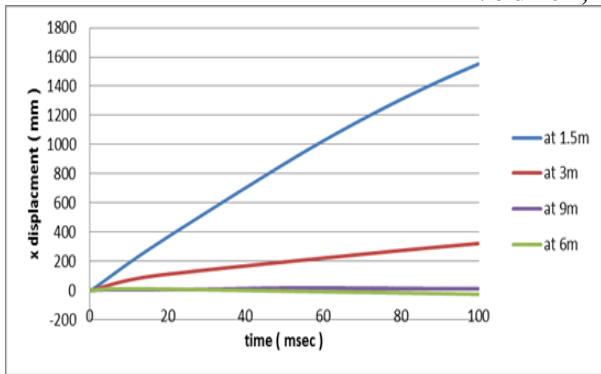


Fig.17: x-displacement histories of at mid height of column C1 of building B – load case 2.

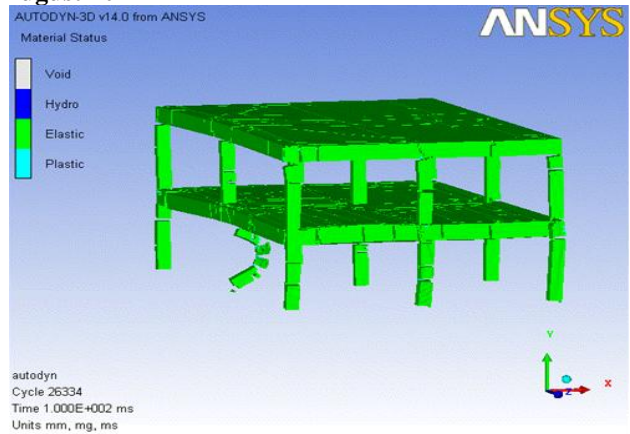


Fig.19: deformed shape of building C due to blast load at 1.5m from the middle column.

Fig.18 shows the variation of transverse z displacement of column C2 with time. Non-linear relationship between time and displacement is observed in this case. The decay of pressure values is more pronounced in case of far blast charge (9 m stand-off distance case) for which the pressure values tend to decrease after short time. This can be attributed to the indirect nature of this pressure resulting from the reflected wave and the relatively long distance from C1. It is shown that the displacement of this column varied from 181.3, 108, 18.5 and 2.8 mm where its displacements in building A are 824.4, 544, 139 and 29.2 mm and in building B are 394.4, 352.7, 140.4 and 34.6 mm. It is shown that the displacement of this column decreasing with increasing aspect ratio of the building as, in this case, the distance between the column and the blast becomes more.

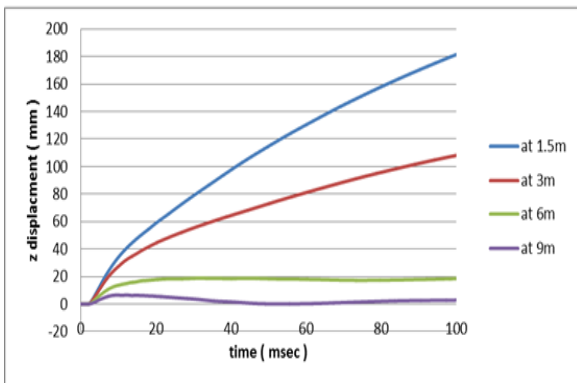


Fig.18: z-displacement histories of at mid height of column C2 of building B – load case 2.

### 3. BUILDING C

For building C, aspect ratio is changed to 1.5 by increasing the breadth of the building (L=9.0m), while the same depth (D=6.0m) is used. The effect of blast is investigated for all previously defined positions and stand-off distances.

#### CASE 1(SYMMETRIC LOADING)

Fig.19 shows the deformed shape of the building C under the effect of the blast load at 1.5 m from the center of middle column. It is shown that there is a total failure in column C2 where the effect of the blast load on this building on column C1 and C2 is less than its effect on building A and B.

Fig.20 shows the variation of transverse z-displacement of column C1 with time. It is observed that the displacement of this column varied from 218, 225, 136 and 65 mm. the corresponding values of displacements in building A are 784, 544, 139 and 29.2 mm and in building B are 394.4, 352.7, 140.4 and 34.6 mm. It is shown that the displacement of this column decreases with increasing the aspect ratio of the building. It is shown also that the displacements of this column in the three buildings are almost equal with increasing the distance of the blast load from the building.

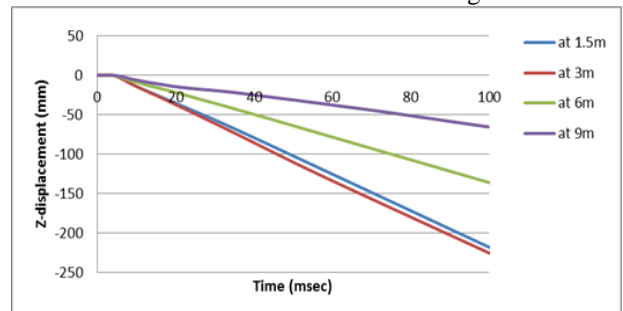


Fig.20: z-displacement histories of at mid height of column C1 of building C – load case 1.

Fig.21 shows the variation of x displacement of column C2 with time. It is shown that the displacements of this column are equal in the three buildings. Pressure values are observed to be approximately the same for case of long stand-off (6 and 9m) which have very small values compared to the near stand-off cases (1.5 and 3m).

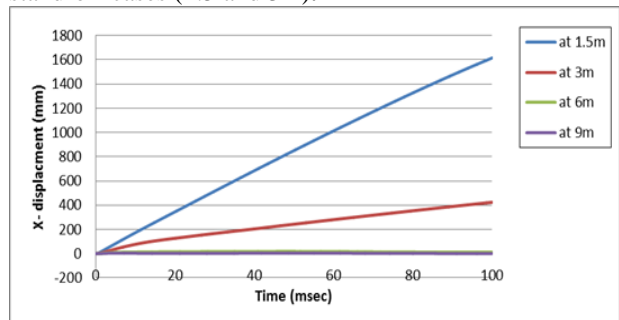
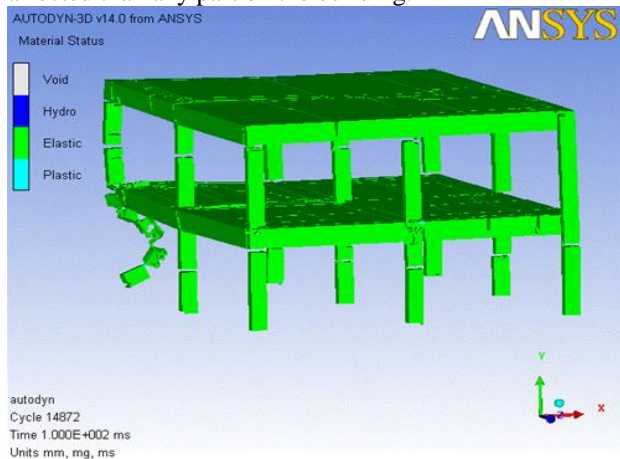


Fig.21: x-displacement histories of at mid height of column C2 of building C – load case 1.

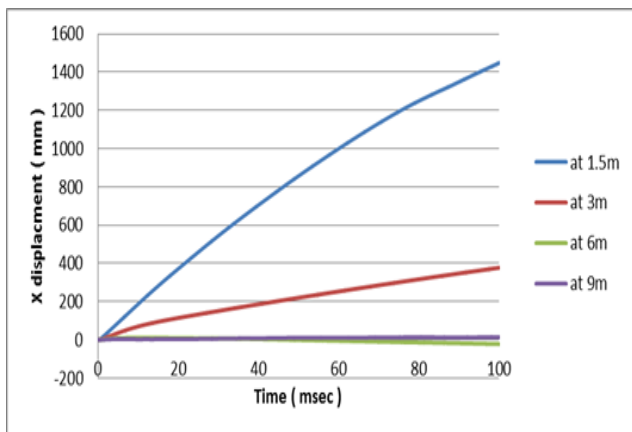
**CASE 2(SKEW LOADING)**

Fig.22 shows the deformed shape of building C under the effect of the blast load at 1.5 m from the building. It is shown that the corner columns in first and second floor are more affected than any part on the building.



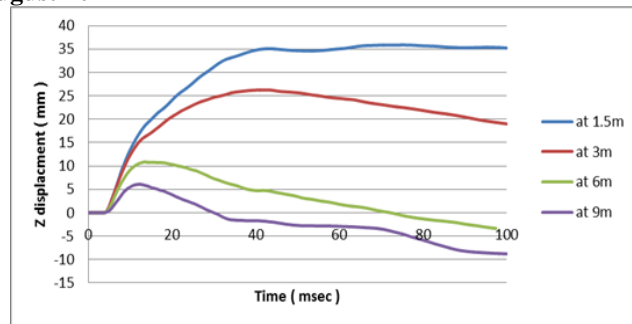
**Fig.22:deformed shape of building C due to blast load at 1.5m from the corner column.**

Fig.23 shows the variation of x displacement of column C1 with time. It is shown that the displacements of this column have approximately the same values in the three buildings, where its displacement in building A are 1583, 387, -1.83, -41.5 , in building B are 1552.5, 321.1, -26.4, 12.05 and in building C are 1450, 377.1 , -21.9, 13.8mm due to blast load at 1.5, 3.0, 6.0 and 9.0m respectively



**Fig.23: x-displacement histories of at mid height of column C1 of building C – load case 2.**

Fig.24 shows the variation of z displacement of column C2 with time. The nonlinear behavior is more clear in all cases of stand-off separation as a result of the building being relatively wide. Decay of the pressure values is observed for all cases such that the pressure values changed sign (direction) for distances of 6 and 9m. It is shown also that the displacement of this column is less than its displacement in building A and B.



**Fig.24: z-displacement histories of at mid height of column C2 of building C – load case 2.**

**V. CONCLUSION**

The responses of three buildings with different aspect ratio (depth to breadth) were studied subjected to blast load. Blast loads with the same TNT charge are located at different standoff distances (1.5, 3, 6 and 9 m) and at two different locations (Symmetric and skew positions) are applied to the building. The main conclusions of the study were as follows:

- 1- The reflected overpressure, temperature of different point in the building increase with decrease the standoff distance of the blast load from the building. The arrival time of reflected over pressure and temperature increase with increasing standoff distance.
- 2- The blast load at distance equal 1.5 m from the building made a total failure in the column in the face of the blast load, which the fragments from the failure of the column moving away from the column at distance up to 1.60 m.
- 3- The displacement at different gauges on the building decrease with increasing the distance of the blast load from the building, where the displacement of the middle column decreasing from 1649.3 to 1.71 mm due to detonation point at 1.50 and 9.0 m from the center of this column.
- 4- In case skew loading, the displacement of the column C3 due to detonation point at 3.0 m larger than its displacement due to blast load at 1.50 m due to reflected pressure from the middle column from blast load at 1.50 m is larger than its reflected pressure due to detonation at 3.0 m due to the difference in angle of incidence.
- 5- With variation the aspect ratios of the buildings there is no variation in the displacement of the column in the face of the blast load.
- 6- With increasing the aspect ratios of the buildings the displacement of the column far from the detonation point decreasing, where the displacement of the corner column due to detonation point at 1.50 m from the center of middle column decreasing from 784, 394 and 218 in building with aspect ratio 0.5, 1.0 and 1.5 respectively.

**REFERENCES**

[1] AHMED, Y.M.T ” RESPONSE OF BRIDGE STRUCTURES SUBJECTED TO BLAST LOADS AND PROTECTION TECHNIQUES TO MITIGATE THE EFFECT OF BLAST HAZARDS ON BRIDGES” a thesis presented to The State University of New Jersey (2009).



ISSN: 2277-3754

ISO 9001:2008 Certified

International Journal of Engineering and Innovative Technology (IJET)

Volume 4, Issue 2, August 2014

- [2] Astarlioglu, S and Krauthammer, T “Response of normal-strength and ultra-high-performance fiber-reinforced concrete columns to idealized blast loads” *Engineering Structures* 61 (2014) 1–12.
- [3] Century Dynamics. (2011). ANSYS AUTODYN user manual (Version 14)
- [4] Chen, H, Zhou, H, Fan, H, Jin, F, Xu, Y, Qiu, Y, Wang, P and Xie, W “Dynamic responses of buried arch structure subjected to subsurface localized impulsive loading: Experimental study” *International Journal of Impact Engineering* 65 (2014) 89e101.
- [5] Izzuddin, B.A, Vlassis, A.G, Elghazouli, A.Y and Nethercot, D.A “Progressive collapse of multi-storey buildings due to sudden column loss — Part I: Simplified assessment framework” *Engineering Structures* 30 (2008) 1308–1318.
- [6] Jayasooriya, R, Thambiratnam, D.P, Perera, N.J and Kosse, V “Blast and residual capacity analysis of reinforced concrete framed buildings” *Engineering Structures* 33 (2011) 3483–3495.
- [7] Kelliher, D and Swaby, K.S “Stochastic representation of blast load damage in a reinforced concrete building” *Structural Safety* 34 (2012) 407–417.
- [8] LI, J and HAO, H, “Development of a Simplified Numerical Method for Structural Response Analysis to Blast Load” *Procedia Engineering* 14 (2011) 2558–2566.
- [9] LI, J and HAO, H, “Numerical study of concrete spall damage to blast loads” *International Journal of Impact Engineering* 68 (2014) 41e55.
- [10] Lin, X, Zhang, Y.X and Hazell, P.J “Modelling the response of reinforced concrete panels under blast loading” *Materials and Design* 56 (2014) 620–628.
- [11] Luccioni, B.M, Ambrosini, R.D, Danesi, R.F, "Analysis of building collapse under blast loads" *Engineering Structures* 26 (2004) 63–71.
- [12] McConnell, J.R and Brown, H “Evaluation of progressive collapse alternate load path analyses in designing for blast resistance of steel columns” *Engineering Structures* 33 (2011) 2899–2909.
- [13] Ngo, T, Mendis, P, Gupta, A and Ramsay, J “Blast Loading and Blast Effects on Structures – An Overview” *EJSE Special Issue: Loading on Structures* (2007).
- [14] Sherkar, P “MODELING THE EFFECTS OF DETONATIONS OF HIGH EXPLOSIVES TO INFORM BLAST-RESISTANT DESIGN” the degree of Master of Science presented to the University at Buffalo, State University of New York (2010).
- [15] Shi, Y, Li, Z.X and Hao, H “A new method for progressive collapse analysis of RC frames under blast loading” *Engineering Structures* 32 (2010) 1691–1703.
- [16] Sohel, K.M.A and Liewb, J.Y.R “Behavior of steel-concrete-steel sandwich slabs subject to impact load” *Journal of Constructional Steel Research* 100 (2014) 163–175.
- [17] Stochino, F and Carta, G “SDOF models for reinforced concrete beams under impulsive loads accounting for strain rate effects” *Nuclear Engineering and Design* 276 (2014) 74–86.
- [18] Wua, C, Hao, H and Lub, Y “Dynamic response and damage analysis of masonry structures and masonry in filled RC frames to blast ground motion” *Engineering Structures* 27 (2005) 323–333.
- [19] Zakrisson, B, Wikman, B, Häggblad, H.A “Numerical simulations of blast loads and structural deformation from near-field explosions in air” *International Journal of Impact Engineering* 38 (2011) 597e612.

#### AUTHOR'S PROFILE

**Osman Shallan** "Head of Structural Eng., Faculty of Engineering, Zagazig University".

**Atef Eraky** "Prof. of Structural Eng., Faculty of Engineering, Zagazig University".

**Tharwat Sakr** "Associate Prof., Department of Structural Eng., Faculty of Engineering, Zagazig University".

**Shimaa Emad** "Demonstrator, Department of Structural Eng., Faculty of Engineering, Zagazig University".